

A Geometrical Comparison between Cell Method and Finite Element Method in Electrostatics

M. Heshmatzadeh and G. E. Bridges¹

Abstract: Cell Method, a Finite Formulation technique, is compared in detail with the Finite Element Method (FEM), a differential-based numerical technique. In the finite formulation technique, Poisson's equation is described starting from a topological foundation. The final set of algebraic equations resulting from the two approaches are compared in matrix form. The equivalence of the coefficient matrices is proven for a Voronoi dual mesh and linear shape functions in the FEM. The difference between the source (charge) vectors in the two approaches is described. It is shown that the use of linear shape functions in the FEM is equivalent to the use of a barycentric dual mesh for charge vectors. Also, it is shown that the coefficient matrix derived from a variational technique, FEM, can be interpreted using the simple geometrical concept of a parallel plate capacitor. As an example, a Schottky barrier diode with a non-uniform doping profile is considered. The results demonstrate the differences between the two approaches in the case of a non-zero electric charge density.

Keyword: Cell Method, Electrostatics, Finite Element Method, Numerical techniques, Poisson's Equation.

1 Introduction

In the field of computational electromagnetics, many different numerical techniques have been developed. The aim of most numerical techniques is to accurately estimate the solution of Maxwell's equations in a discretized space and time domain. "The basic idea is to approximate quantities of interest in terms of sampling functions, often polynomials that are then substituted for these quanti-

ties in various analytical operations. Thus integral operators are replaced by finite sums and differential operators are similarly replaced by finite differences", [Miller (1998)].

Maxwell's equations describe fundamental laws (Gauss's law, Faraday's law and Maxwell-Ampère's law) based on experimental observation which are naturally stated in terms of physical variables defined on volumes, surfaces and lines. These laws govern the behavior of the magnetic and electric fields in a specific physical media and can be expressed, although not necessarily, in differential form which is the most common presentation for them. In this case, a limiting process is performed on the finite geometrical objects (lines, surfaces or volumes) and differential equations are thus obtained as a mathematical model for the physical laws. If these differential equations can be solved, the field variables (such as electric and magnetic fields, current density, charge density) will be specified at every point of the space (and/or time) domain. Unfortunately, in almost all cases, the differential equations do not have an analytical solution and have to be solved numerically.

Using a numerical technique, we replace the differential (or integral) equations by finite differences (or finite sums) departing from the limiting process that we had performed to obtain the differential (or integral) equation. If you question why the limiting process is performed in the first place, then Finite Integration Techniques can be considered a more reasonable approach.

Starting from Maxwell's equations in their differential form is the basis for differential-based numerical methods such as Finite Difference Time Domain (FDTD, [Taflöv (1995)]), Finite Element Method (FEM, [Silvester and Ferrari

¹ ECE Department, University of Manitoba, MB, CA.

(1990)) and Transmission Line Matrix (TLM, [Christopoulos (1995)]). On the other hand, starting from the integral form of Maxwell's equations is the basis for Finite Integration Techniques (FIT, [Clemens and Weiland (2001)]).

Cell Method is a numerical technique based on exact discretization of physical laws and on using global (integral) variables. While field variables are a result of performing a limiting process and are defined at every point of the spatial domain, global variables are defined and measurable on their corresponding geometrical elements. For example, when describing "current", it is natural to relate this concept to a "surface" through which the current passes. In performing a limiting process, we eliminate the geometrical element (surface in this case) and the physical concept of current and instead we obtain a field variable (current density) which is now a mathematical concept.

Cell Method is a finite integration technique with respect to its use of global variables. The technique utilizes a two-oriented-grid framework and enables one to formulate physical laws directly as a set of algebraic equations. The original concept of Cell Method was first developed by Tonti [Tonti (2001)]. Since then, Cell Method has been developed, modified and applied to different problems in science and engineering such as: electrostatics [Bettini and Trevisan (2003)], magnetostatics [Repetto and Trevisan (2003), Trevisan and Kettunen (2004)], Eddy currents [Bellina; Bettini; Tonti and Trevisan (2002), Specogna and Trevisan (2005)], and electromagnetics in the time-domain [Marrone and Mitra (2004), Araneo (2002)] and the frequency-domain [Marrone (2002), [Marrone; Frasson and Figueroa (2002), Marrone; Grassi and Mitra (2004)]. Cell Method has also been used in other engineering fields e.g. elastodynamics [Cosmi (2005)], and fluid dynamics, [Straface; Troisi and Gagliardi (2006)]. Theoretical investigations and comparisons between the Cell Method and other numerical techniques [Mattiussi (2000), Bossavit (1998), Bossavit and Kettunen (2000), Marrone (2001)], reveal its natural and rather simple essence.

In the following sections we briefly study physical laws under two main categories: topological

relations and constitutive relations. Electrostatic laws are then formulated in both the differential and the finite frameworks. Cell Method is compared with a variational technique (FEM) in terms of the final coefficient matrix and source vectors. It is shown that even though FEM doesn't explicitly use a dual mesh, the resulting coefficient and source matrices represent Voronoi and barycentric dual meshes, respectively.

2 Physical Laws as Topological Relations

Physical laws are the result of consistent observations and experiments. The great similarity between physical laws in different physical fields (which seems amazing!) is an important fact supporting the idea: discovering a physical law requires finding, defining and fitting proper physical variables to a topological relation which by itself doesn't involve any specific physical quantity. Due to the historical evolution of physics and mathematics, topological relations have been expressed in a differential-integral form (e.g. Stokes and Divergence theorems), however, they can be expressed directly and exactly in a finite framework, [Mattiussi (2000)]. For a brief description of finite topological relations consider Fig.1 and the following notation and definitions for directed three dimensional geometrical objects:

1. V_γ is an arbitrary volume in the spatial domain and its boundary is a closed surface, S : $\partial(V_\gamma) = S$, $\partial(S) = 0$. We can define a direction for V_γ arbitrarily as being either a source (outward to its closed surface) or a sink.
2. S_β is an arbitrary surface in the spatial domain and its boundary is a closed line, L : $\partial(S_\beta) = L$, $\partial(L) = 0$. We can define a direction for S_β arbitrarily along its closed boundary.
3. L_α is an arbitrary line in the spatial domain and its boundary is a set of two directed points, P : $\partial(L_\alpha) = P$, $\partial(P) = 0$. We can define a direction for L_α arbitrarily from one boundary point to the other.
4. P_i is an arbitrary point in the spatial domain

and we can define a positive direction for P_i arbitrarily as being either a sink or a source.

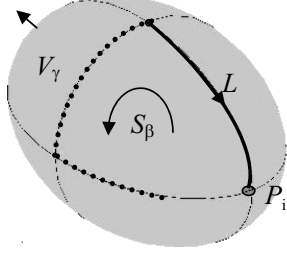


Figure 1: Geometrical objects and their closed boundaries.

Now we define the following generic global variables as *linear* functions operating on the geometrical objects:

$K(V_\gamma)$ on volumes,
 $\Phi(S_\beta)$ on surfaces,
 $V(L_\alpha)$ on lines,
 $\phi(P_i)$ on points.

The linearity property,

$$F(aX_i + bX_j) = aF(X_i) + bF(X_j),$$

where F is a global variable defined on the geometrical object X , and a and b are scalars, allows us to add global variables on the corresponding geometrical objects and define topological relations.

2.1 Topological relations

Topological relations linearly (e.g. up to a scaling factor) relate the global variable on any geometrical object (except points) to the global variable defined on its boundary as

$$V(L_\alpha) = a_G \phi(\partial L_\alpha), \quad (1.a)$$

$$\Phi(S_\beta) = a_C V(\partial S_\beta), \quad (1.b)$$

$$K(V_\gamma) = a_D \Phi(\partial V_\gamma), \quad (1.c)$$

where a_G , a_C , and a_D are scaling factors. To illustrate the three relations in (1), consider the following examples.

2.1.1 Gradient relation

Given the global variable on points as shown in Fig. 2, we can define the global variable on lines as in 1.a ($a_G = -1$):

$$V(L_1) = -(-\phi(P_1) + \phi(P_3))$$

$$V(L_2) = -(-\phi(P_1) + \phi(P_2))$$

$$V(L_3) = -(\phi(P_2) - \phi(P_3))$$

$$\text{or } \bar{V} = -G \cdot \bar{\phi} \quad (2.a)$$

where ‘ \cdot ’ denotes matrix multiplication and \bar{V} and $\bar{\phi}$ are column vectors. Matrix G is the finite equivalent of the gradient operator and represents the topological relation between directed points and lines as

$$G_{\alpha i} = \begin{cases} 0; & \text{if point } i \text{ is not a face of line } \alpha. \\ 1; & \text{if point } i \text{ is a face of line } \alpha \text{ with the same direction.} \\ -1; & \text{if point } i \text{ is a face of line } \alpha \text{ with the opposite direction.} \end{cases}$$

where a ‘‘face’’ for a line is any of its boundary points.

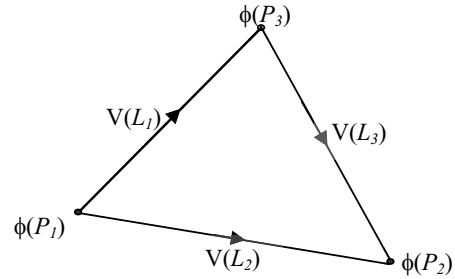


Figure 2: Topological relation between lines and points.

2.1.2 Curl relation

Given the global variable on lines as shown in Fig. 3, we can define the global variable on surfaces as in 1.b ($a_C = 1$):

$$\Phi(S_1) = V(L_2) - V(L_3) + V(L_5)$$

$$\Phi(S_2) = -V(L_1) - V(L_4) - V(L_5)$$

$$\text{or } \bar{\Phi} = C \cdot \bar{V}, \quad (2.b)$$

where $\bar{\Phi}$ is a column vector. Matrix C is the finite equivalent of the curl operator and represents the topological relation between directed surfaces and lines as

$$C_{\beta\alpha} = \begin{cases} 0; & \text{if line } \alpha \text{ is not a face of surface } \beta. \\ 1; & \text{if line } \alpha \text{ is a face of surface } \beta \text{ with the same direction.} \\ -1; & \text{if line } \alpha \text{ is a face of surface } \beta \text{ with the opposite direction.} \end{cases}$$

where a “face” for a surface is any of its boundary lines.

As an exercise, we can start from the values on the points in Fig. 2 and obtain the finite equivalent of the vector analysis identity ($\nabla \times \nabla \phi \equiv 0$) as

$$\bar{V} = -G \cdot \bar{\phi}, \quad \bar{\Phi} = C \cdot \bar{V} \Rightarrow \bar{\Phi} = -C \cdot (G \cdot \bar{\phi}) = 0,$$

$$C \cdot G \equiv 0.$$

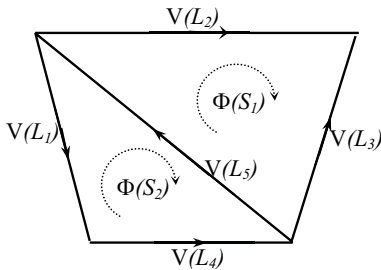


Figure 3: Topological relation between surfaces and lines.

2.1.3 Divergence relation

Given the global variable on surfaces as shown in Fig. 4, we can define the global variable on volumes as in 1.c ($a_D=1$):

$$K(V_1) = \Phi(S_1) + \Phi(S_2) - \Phi(S_3) + \Phi(S_4)$$

$$\text{or } \bar{K} = D \cdot \bar{\Phi}, \tag{2.c}$$

where \bar{K} is a column vector. Matrix D is the finite equivalent of the divergence operator and represents the topological relation between directed

volumes and surfaces as

$$D_{\gamma\beta} = \begin{cases} 0; & \text{if surface } \beta \text{ is not a face of volume } \gamma. \\ 1; & \text{if surface } \beta \text{ is a face of volume } \gamma \text{ with the same direction.} \\ -1; & \text{if surface } \beta \text{ is a face of volume } \gamma \text{ with the opposite direction.} \end{cases}$$

where a “face” for a volume is any of its boundary surfaces.

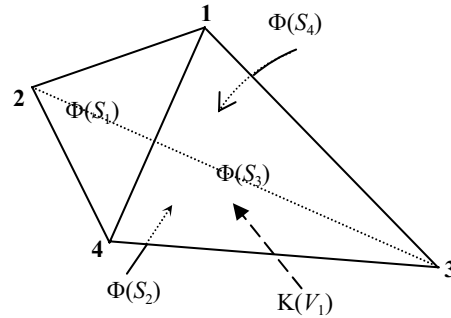


Figure 4: Topological relation for volumes and surfaces. The surfaces are directed as: $S_1(1,2,4)$, $S_2(2,3,4)$, $S_3(1,3,4)$, $S_4(1,3,2)$. The volume is directed as a source.

As an exercise, we can start from some values on the lines in Fig. 4 and obtain the finite equivalent of the vector analysis identity ($\nabla \cdot (\nabla \times A) \equiv 0$) as

$$\bar{\Phi} = C \cdot \bar{V}, \quad \bar{K} = D \cdot \bar{\Phi} \Rightarrow \bar{K} = D \cdot (C \cdot \bar{V}) = 0,$$

$$D \cdot C \equiv 0.$$

Relations 1.a, 1.b, 1.c, are the finite equivalence of the “Fundamental Integration Theorem”, “Stokes Theorem”, and “Divergence Theorem”, specified by the incidence matrices, G, C, D, respectively. They do not contain any material and metric information. To solve a physical problem, in addition to topological relations, we also need “physical links” between variables which contain medium and metric information. These links are usually called “constitutive relations” [Mattiussi (2000)].

2.2 Constitutive relations

Having the spatial domain divided into a (primal) mesh consisting of geometrical objects, proper

global variables can be defined and topological relations stated. To use global primal variables to describe a real physical system requires defining a set of “dual” variables and forming a physical-based relation between primal and dual variables. For example, the variables defined on primal surfaces (fluxes) are related to the variables defined on dual lines (voltages). This relation is where all material and metric-dependent information appear. To formulate constitutive relations, we need to define a dual mesh. The minimal requirement to construct a dual mesh is:

For any primal (dual) volume, $V_\gamma(\tilde{V}_i)$, there is one and only one dual (primal) point, $\tilde{P}_\gamma(P_i)$. For any primal (dual) surface, $S_\beta(\tilde{S}_\alpha)$, there is one and only one dual (primal) line, $\tilde{L}_\beta(L_\alpha)$.

The correspondence between primal and dual variables can be described as

$$\tilde{P}_\gamma \leftrightarrow V_\gamma, \quad \tilde{L}_\beta \leftrightarrow S_\beta, \quad \tilde{S}_\alpha \leftrightarrow L_\alpha, \quad \tilde{V}_i \leftrightarrow P_i$$

The dual geometrical objects for the primal mesh in Fig. 1 are shown in Fig. 5.

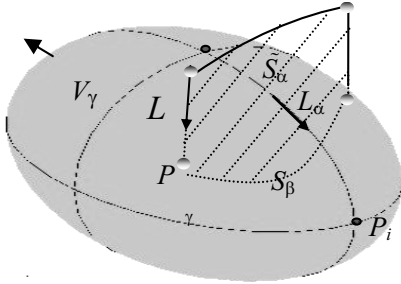


Figure 5: Dual geometrical objects for primal geometrical objects in Fig. 1. The dual volume for the primal point (P_i) is not shown.

With the given definition for duality, it is easy to show [Tonti (2001)] the following relations between incidence matrices for primal and dual meshes:

$$\tilde{G} = -D^t, \quad \tilde{C} = C^t, \quad \tilde{D} = -G^t,$$

where superscript t denotes transpose operator and G, C and D are Gradient, Curl and Divergence incidence matrices for the dual mesh. The same

topological relations as (2) are also valid for the dual geometrical objects as

$$\bar{F} = \tilde{G} \cdot \bar{N}, \quad (3a)$$

$$\bar{\Psi} = \tilde{C} \cdot \bar{F}, \quad (3b)$$

$$\bar{Q} = \tilde{D} \cdot \bar{\Psi}, \quad (3c)$$

where \bar{N} , \bar{F} , $\bar{\Psi}$, \bar{Q} are the column vectors containing the global variables defined on the dual points, lines, surfaces and volumes, respectively.

With definition of eight global variables on primal and dual geometrical objects and 6 topological relations (2, 3) we still need two more relations to be able to solve for any global variable.

The link between the variables for the primal lines and the variables for the dual surfaces (and vice-versa) embody the physical system they are used to describe, and are called constitutive relations.

Constitutive equations can be approximately expressed as a mapping from the space of V to the space of Ψ , and from the space of Φ to the space of F as

$$\begin{aligned} \bar{\Psi}(\tilde{S}) &= M_\epsilon \bar{V}(L), \\ \bar{\Phi}(S) &= M_\mu \bar{F}(\tilde{L}), \end{aligned} \quad (4)$$

where M_ϵ and M_μ are constitutive matrices.

In contrast to the exact and physically independent nature of the topological relations, constitutive matrices are dependent on physical properties of the material, construction of the dual mesh, metric and direction. In a physical link between global variables (as scalar numbers) all the above information are included in the constitutive matrices. The results of experiment and measurement on a defined physical system have to be fit in the finite matrix forms of (4). In (4), global variables defined on surfaces (fluxes) are considered as scalar numbers with an implicit direction given to them as the normal to the surface. It is based on the physical concept of “passing through a surface” which automatically includes only the normal component of a directional flow. The mathematical interpretation of the above concept is expressed using field variables (e.g. magnetic flux density) as the inner product of a flow and the normal to the surface (e.g. $\iint B \cdot ds$).

Specific choices for the dual mesh might result in simple mapping functions from the primal variables to the dual variables. For example, if the physical link is a relation between fluxes (which implicitly means normal flux) through the primal surfaces and voltages on the dual lines in an isotropic linear media, an orthogonal dual mesh (if possible) results in diagonal constitutive matrices. For a non-orthogonal dual mesh, knowing the value of the flux through a primal surface is not enough to obtain the voltage on the dual line and an averaging procedure is needed using the neighbor fluxes. The resulting constitutive matrix is therefore non-diagonal.

To understand how we can apply the discussed finite framework to solve a real physical problem, we study the electrostatic case as an example in the following section.

3 Electrostatic laws

Electrostatic laws are the statement of relations between global electromagnetic quantities when $d/dt \rightarrow 0$ and are known as: Faraday's law, Gauss's law and the electric constitutive relation. We now study these laws in both the finite and the differential frameworks.

3.1 Faraday's law

In its general time dependent form, Faraday's law is a curl relation (1.b) and relates the value of changes (in time) in magnetic flux, Φ , for a surface, S , to the value of the electric voltage, V , on the boundary of the surface, ∂S . Since the time variation of magnetic flux is zero in electrostatics; the electrostatic Faraday's law states:

“The electric voltage for any closed line is zero.”

3.1.1 Finite formulation

Using global variables on the primal geometrical objects, Faraday's law in electrostatic is

$$\Phi(S_\beta) = V(L) = 0; \quad L = \partial S_\beta. \quad (5)$$

Definition of a global variable on primal points (electric potential, ϕ) guarantees that the value of

Φ is zero for all surfaces. This yields the equivalent gradient form of Faraday's law as

$$\bar{V} = -G \cdot \bar{\phi} \quad (2.a)$$

The minus sign is the scaling factor in (1.a) due to experimental convention. Fig. 6 illustrates Faraday's law.

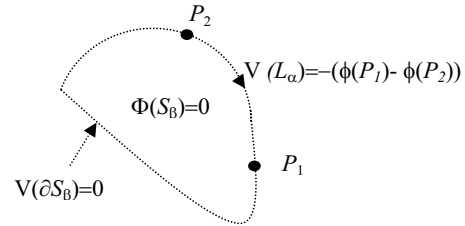


Figure 6: Faraday's law for the surface, S_β , enclosed by the line, ∂S_β .

3.1.2 Differential formulation

Differential equations are the result of performing a limiting process on global variables and using field variables. Based on the defined global variables in (1), we can obtain electric field intensity as

$$E \triangleq \lim_{L_\alpha \rightarrow 0} \frac{V}{L_\alpha} \quad (6)$$

and results in a differential expression of Faraday's law :

$$E = -\nabla\phi \Leftrightarrow \oint E \cdot dl = 0, \quad (7)$$

where ∇ is the gradient operator.

3.2 Gauss's law

Gauss's law is a balance or divergence relation (1.c) and relates the value of the charge, Q , in a volume, \tilde{V}_i , to the value of the electric flux, $\tilde{\Psi}$ passing through the boundary of the volume, $\partial\tilde{V}_i$. The electrostatic Gauss's law states:

“The electric flux leaving a closed surface is equal to the electric charge in the volume enclosed by the surface.”

3.2.1 Finite formulation

Using global variables on the dual geometrical objects, Gauss's law is written as:

$$Q(\tilde{V}_i) = \Psi(\tilde{S}); \quad \tilde{S} = \partial\tilde{V}_i, \quad (8)$$

or in its equivalent matrix form

$$\bar{Q} = \bar{D} \cdot \bar{\Psi}. \quad (9)$$

The scaling factor is equal to one in (1.c) due to experimental convention. Fig. 7 illustrates Gauss's law.

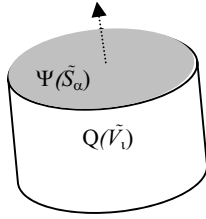


Figure 7: Gauss's law for a volume, \tilde{V}_i , enclosed by the surface, $\partial\tilde{V}_i$.

3.2.2 Differential formulation

Performing a limiting process on the defined global variables, (3), we obtain electric charge density and electric flux density, respectively, as

$$\rho = \lim_{\tilde{V}_i \rightarrow 0} \frac{Q}{\tilde{V}_i}, \quad D = \lim_{\tilde{S}_\alpha \rightarrow 0} \frac{\Psi}{\tilde{S}_\alpha}, \quad (10)$$

which results in the differential form of Gauss's law:

$$\rho = \nabla \cdot D \Leftrightarrow \iiint_{\partial\tilde{V}} D \cdot ds = \iiint_{\tilde{V}} \rho dv, \quad (11)$$

where $\nabla \cdot$ is the divergence operator.

3.3 Constitutive relation

The electrostatic constitutive relation is a relation between the electric voltage and the electric flux in a specific physical media. For simple isotropic linear media, as defined in Harrington (1961), this relation reduces to a number relating the electric flux through a surface to the electric voltage on

the line normal to the surface. Since this relation is found experimentally and involves global variables, it can be approximated directly (not uniquely) in a finite form as

$$\frac{\Psi(\tilde{S}_\alpha)}{|\tilde{S}_\alpha|} = \varepsilon \frac{V(L_\alpha)}{|L_\alpha|} \Rightarrow M_\varepsilon(\alpha, \alpha) = \varepsilon \frac{|\tilde{S}_\alpha|}{|L_\alpha|}, \quad (12)$$

where ε is the permittivity of the homogeneous media around the line, L_α , and its orthogonal dual surface, \tilde{S}_α , as shown in Fig. 8. $|A|$ refers to the length, area or volume of the geometrical object, A .

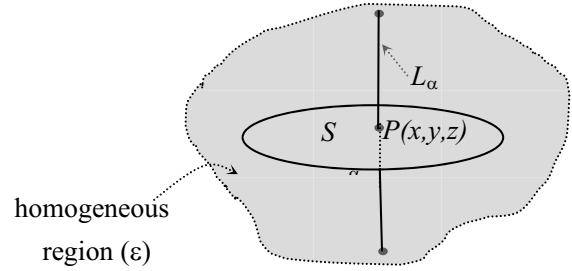


Figure 8: Electric constitutive relation for a homogeneous region and orthogonal primal-dual line-surface configuration.

Performing a limiting process on (12), we eliminate the physical concept of the geometrical objects and obtain field variables, electric field intensity, E , and electric flux density, D , which are defined at all points in the spatial domain. The differential form of the electrostatic constitutive relation then becomes:

$$D = \lim_{\tilde{S}_\alpha \rightarrow 0} \frac{\Psi(\tilde{S}_\alpha)}{\tilde{S}_\alpha}, \quad E = \lim_{L_\alpha \rightarrow 0} \frac{V(L_\alpha)}{L_\alpha}, \quad (13)$$

$$D(x, y, z) = \varepsilon E(x, y, z). \quad (14)$$

Here ε is the permittivity of the infinitesimal volume around the point $P(x, y, z)$.

3.4 Poisson's equation

Using global variables and finite formulation, (2.a, 4, 9), we obtain the finite form of Poisson's equation as

$$G^t \cdot M_\varepsilon \cdot G \cdot \bar{\phi} = \bar{Q}. \quad (15)$$

The differential expression of electrostatic laws (7, 11, 14) results in the familiar form of Poisson's equation as

$$\nabla \cdot \epsilon \nabla \phi = -\rho. \quad (16)$$

4 Numerical approach

The finite form of Poisson's equation, (15), is applicable to a discretized spatial domain directly and results in a set of algebraic equations. In cases with no exact analytic solution (almost all cases), however, numerical techniques are needed to solve the differential form (16) which, after the appropriate discretization, also lead to a set of algebraic equations. In the next section, we compare a finite formulation (Cell Method) with a differential-based formulation (FEM) for solving Poisson's equation on a 2-D geometry. In the 2-D case an extruded mesh of triangles (elements) is used as shown in Fig. 9. The resulting duality relations in this case are reduced to

$$P_i \leftrightarrow \tilde{S}_i, \quad L_\alpha \leftrightarrow \tilde{L}_\alpha, \quad S_\beta \leftrightarrow \tilde{P}_\beta. \quad (17)$$

Note that the 2D triangular surface, S_β , is also referred to as element e , which is the common notation for the Finite Element Method.

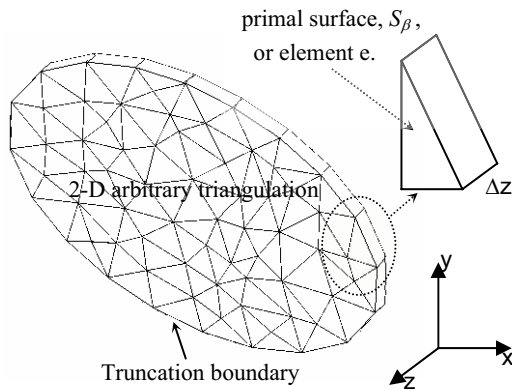


Figure 9: Extruded 2-D geometry with $\Delta z = 1$ unit length.

4.1 Permittivity and charge functions

The differential expression of physical laws has automatically led us to convert global variables

and measurement results into a differential framework. Although material properties (e.g. ϵ , μ , σ) and charge density (ρ) are found experimentally in real problems, the results are expressed as continuous functions in the spatial domain. Differential-based numerical techniques have adapted many different schemes to average or interpolate the given continuous functions and discretize them for the given spatial mesh. Even when working in a finite framework, we are usually forced to use the given continuous functions which are strongly dependent on the resolution of measurements and experiments. If the resolution of the measurements is high enough with respect to our discrete domain, we can accept the data as a continuous function. However, even in this case, a weighted *integral* of the continuous functions on the proper geometrical object is all that is required. If the resolution of measurements is the same as the discrete domain, we can define discontinuous functions which are constant on primal or dual elements. This suggests, as shown in Fig. 10, that material properties or charge density can be defined as constant numbers (averaged quantities) for geometrical elements in the computational mesh.

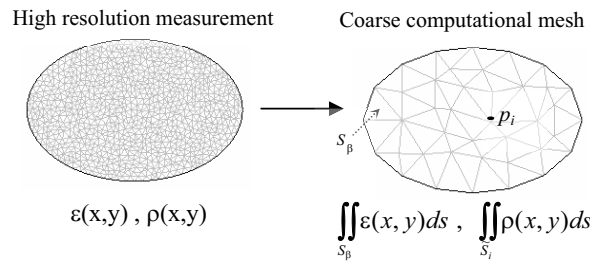


Figure 10: Continuous functions used for defining averaged quantities in the discrete domain.

4.2 Finite formulation

To solve the finite form of Poisson's equation, (15), we consider the 2-D triangular mesh, as shown in Fig. 9, as the primal mesh. The gradient matrix (the incidence matrix between primal lines and points) can then be constructed and is material and metric-free. To obtain the constitutive matrix, M_e we need to first define the dual mesh.

An orthogonal dual mesh (Delaunay-Voronoi) is considered here as shown in Fig. 11. The dual points are the circumcenter of the triangles and we assume there is no obtuse triangle in our primal mesh. A diagonal constitutive matrix, M_ϵ is then constructed as in (12).

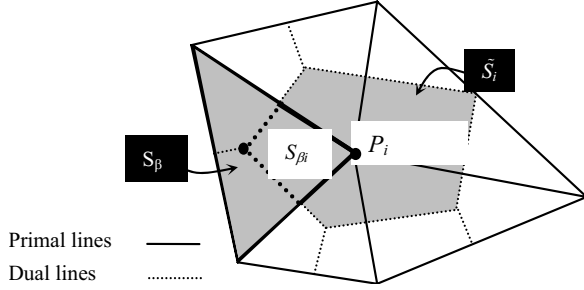


Figure 11: A Delaunay-Voronoi dual mesh where the dual points are the circumcenter of the primal surfaces.

The final finite form of (15) can be rewritten as

$$C_{FF}\bar{\Phi} = Q_{FF}, \quad (18)$$

where $C_{FF} = G^t M_\epsilon G$. Q_{FF} is the column vector containing the total charges enclosed in the dual volumes (extruded surfaces around primal points). This column vector can be found by sampling the given charge density function at primal points (or measuring the total charge in dual surfaces). To have a consistent comparison with the FEM approach, we assume a constant charge density, ρ_β , for each primal element (S_β or e). The column vector for electric charge in this case is found as

$$Q_{FF}(i) = \sum_{\beta} \rho_\beta S_{\beta i}, \quad (19)$$

where $S_{\beta i}$ is as indicated in Fig. 11, and the sum is taken over all primal triangles, S_β sharing the primal point P_i .

It should be noted that multiplying the constitutive matrix, M_ϵ , in the form of $G^t M_\epsilon G$, results in assembling the n by n coefficient matrix, C_{FF} , which

can be constructed directly as

$$C_{FF}(i,j) = \begin{cases} 0; & \text{if } P_i \text{ and } P_j \text{ are} \\ & \text{not connected.} \\ -\bar{\epsilon}_\alpha \frac{|\tilde{S}_\alpha|}{|L_\alpha|} = -\bar{\epsilon}_\alpha \frac{|\tilde{L}_\alpha|}{|L_\alpha|}; & \text{if } i \neq j \text{ and } P_i \text{ \&} \\ & P_j \text{ are connected.} \\ \sum_k C_{FF}(i,k); & i = j \text{ and} \\ & k = 1 \dots n, k \neq i. \end{cases} \quad (20)$$

where n is the total number of primal points. The assumption of having a constant permittivity for each primal element is made here. Note that the matrix elements are equivalent to that of a parallel plate capacitor between two primal points P_i and P_j as shown in Fig. 12. The average permittivity ($\bar{\epsilon}_\alpha$ related to the line L_α (connecting the points P_i and P_j)) is calculated in the following section.

4.2.1 Average permittivity

An averaging scheme is used to define the permittivity related to primal lines at the interface between two different materials as shown in Fig. 12.

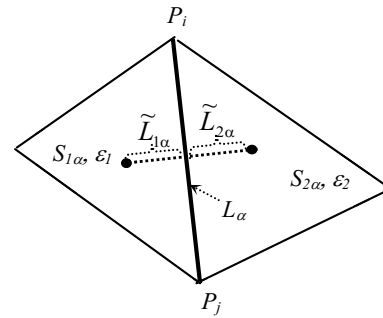


Figure 12: A primal line L_α on the interface of two different materials.

Calculation of the average permittivity is based on the continuity of the global variables (electric flux for dual extruded surfaces and electric voltage for

primal lines) as follows:

$$\begin{aligned} \frac{\Psi(\tilde{S}_\alpha)}{|\tilde{S}_\alpha|} &= \bar{\epsilon}_\alpha \frac{V(L_\alpha)}{|L_\alpha|} \Rightarrow M_\epsilon(\alpha, \alpha) = \bar{\epsilon}_\alpha \frac{|\tilde{S}_\alpha|}{|L_\alpha|} \\ \Psi(\tilde{S}_\alpha) &= \Psi(\tilde{S}_{1\alpha}) + \Psi(\tilde{S}_{2\alpha}) \\ &= \epsilon_1 |\tilde{S}_{1\alpha}| \frac{V(L_\alpha)}{|L_\alpha|} + \epsilon_2 |\tilde{S}_{2\alpha}| \frac{V(L_\alpha)}{|L_\alpha|} \quad (21) \\ \frac{\Psi(\tilde{S}_\alpha)}{|\tilde{S}_\alpha|} &= \frac{\epsilon_1 |\tilde{S}_{1\alpha}| + \epsilon_2 |\tilde{S}_{2\alpha}|}{|\tilde{S}_\alpha|} \frac{V(L_\alpha)}{|L_\alpha|} \\ \Rightarrow \bar{\epsilon}_\alpha &= \frac{\epsilon_1 |\tilde{L}_{1\alpha}| + \epsilon_2 |\tilde{L}_{2\alpha}|}{|\tilde{L}_\alpha|}. \end{aligned}$$

4.3 Finite element approach

The Finite Element Method is a variational technique that finds the stationary point of a functional in order to solve a differential equation, $\mathfrak{L}\phi = q$, where \mathfrak{L} is a positive-definite and self-adjoint differential operator [Silvester and Ferrari (1990)]. The functional for the homogenous Poisson's equation, which is related to the total energy in the system (W), is minimized at the solution of the differential equation [Sadiku; Makki and Agba (1991)]

$$\begin{aligned} \nabla^2 \phi &= -\frac{\rho}{\epsilon} \Leftrightarrow \\ W_{\min} = W(f = \phi) &= \frac{1}{2} \iiint_V \left[\epsilon |\nabla \phi|^2 - 2\rho\phi \right] dv, \quad (22) \end{aligned}$$

where f is the generic variable for the energy functional, W . With the assumption of a 2-D extruded mesh as the solution region, V , the volume integral reduces to the sum of surface integrals over the area of each triangular element, e , as was shown in Fig. 9.

In the numerical procedure for minimizing W , the unknown potential distribution, $\phi(x, y)$, is approximated in the discretized spatial domain. The known functions, $\epsilon(x, y)$ and $\rho(x, y)$, may be also approximated to maintain a reasonable computational expense. Here we have used a uniform charge density, ρ_e , and permittivity, ϵ_e , for each element and a linear interpolation function for the

unknown potential over each element as

$$\phi_e = \sum_{i=1}^3 \phi_{ei} \alpha_i(x, y), \quad (23)$$

where $\alpha_i = A_i/A_e$ is the shape function associated with vertex P_i , and A_i and A_e are as in Fig. 13.

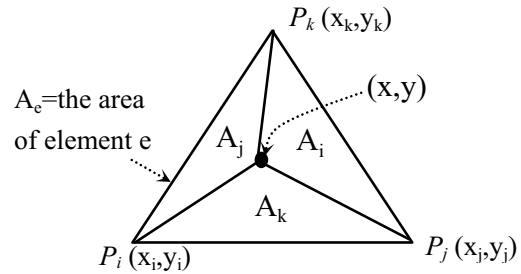


Figure 13: A typical triangular element, e , and associated linear shape functions.

Using (23), the total energy for element e can be written in a matrix form as

$$W_e = \frac{1}{2} \bar{\phi}_e^T C_e \bar{\phi}_e - T_e \bar{\phi}_e, \quad (24)$$

where $\bar{\phi}_e$ is the column vector containing the unknown potentials at the vertices of element e , and C_e is the square element stiffness matrix defined as [Sadiku; Makki and Agba (1991)]

$$C_e(i, j) = \int_{A_e} \epsilon_e \nabla \alpha_i \cdot \nabla \alpha_j dA = \frac{\epsilon_e}{4A_e} (X_i X_j + Y_i Y_j), \quad (25)$$

where

$$\begin{aligned} X_1 &= x_3 - x_2, & X_2 &= x_1 - x_3, & X_3 &= x_2 - x_1, \quad (26) \\ Y_1 &= y_3 - y_2, & Y_2 &= y_1 - y_3, & Y_3 &= y_2 - y_1. \end{aligned}$$

In (24) T_e is a row vector representing the weighting of each vertex in summing the total charge in element e as

$$T_e(i) = \rho_e \iint_{A_e} \alpha_i ds = \rho_e A_e / 3. \quad (27)$$

By applying (24) to all elements in the solution region, we obtain the total energy per unit length

for the whole region with N elements and n nodes as:

$$W = \sum_{e=1}^N W_e = \frac{1}{2} \vec{\Phi}^T C_{FEM} \vec{\Phi} - T_{FEM} \vec{\Phi}, \quad (28)$$

where C_{FEM} and T_{FEM} are the final assembled matrices.

Minimizing (28) with respect to the n unknowns, ϕ_i , results in the following final matrix equation:

$$C_{FEM} \vec{\Phi} = Q_{FEM}. \quad (29)$$

Here Q_{FEM} is the n by one charge vector and is defined as

$$Q_{FEM}(i) = \sum_{\beta} \rho_{\beta} S_{\beta} / 3 = \sum_{\beta} \rho_{\beta} S_{\beta i}, \quad (30)$$

where the sum is taken over all elements, S_{β} , sharing the node P_i as in Fig. 14. This is equivalent to the use of a barycentric dual mesh.

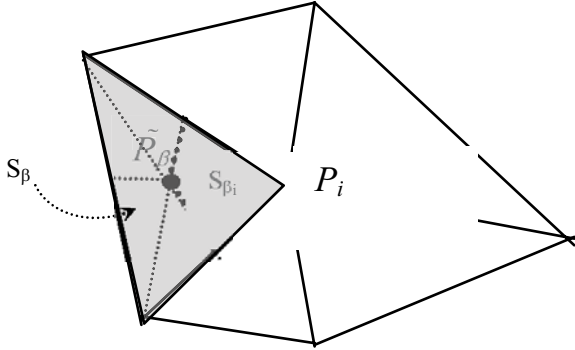


Figure 14: Calculation of Q_{FEM} based on a constant charge density in each triangle which represents a barycentric dual mesh. The dotted lines are the medians of the element S_{β} and \tilde{P}_{β} is its barycenter (centroid).

4.4 Comparison of Cell Method and FEM

Two systems of algebraic equations (18, 29) were obtained from the Finite Formulation and Finite Element Method approaches, respectively. To investigate the differences and similarities between the two methods, we study coefficient matrices, C_{FEM} and C_{FF} , and charge vectors, Q_{FEM} and Q_{FF} , separately.

4.4.1 Coefficient matrices

Considering Fig. 15 and the element stiffness matrix in FEM (25) it can be seen that

$$C_e(i, j) = \frac{\epsilon_e}{4A_e} (X_i X_j + Y_i Y_j) = \epsilon_e \frac{-\vec{AC} \cdot \vec{CB}}{2 |\vec{AC} \times \vec{CB}|} \quad (31)$$

Assuming angle $C \leq 90^\circ$ and $i \neq j$

$$C_e(i, j) = \epsilon_e \frac{-|AC| \cdot |BC| \cos \hat{C}}{2 |AC| \cdot |BC| \sin \hat{C}} = \epsilon_e \frac{-\cot \hat{C}}{2}. \quad (32)$$

For $i = j$

$$\begin{aligned} C_e(i, i) &= \frac{\epsilon_e}{4A_e} (X_i X_i + Y_i Y_i) = \epsilon_e \frac{-\vec{BC} \cdot \vec{CB}}{2 |BC| \cdot |AH|} \\ &= \epsilon_e \frac{|BC|}{2 |AH|} = \epsilon_e \frac{|BH| + |HC|}{2 |AH|} \\ &= -\epsilon_e \left(\frac{\cot \hat{B}}{2} + \frac{\cot \hat{C}}{2} \right) \\ &= -(C_e(i, k) + C_e(i, j)). \end{aligned} \quad (33)$$

To compare the element matrix C_e with the element matrix C_{FF} , consider the circumcircle of the element e as shown in Fig. 15. It is seen that

$$\begin{aligned} \hat{C} = \hat{O} &\Rightarrow C_e(i, j) = -\epsilon_e \frac{\cot \hat{C}}{2} = -\epsilon_e \frac{\cot \hat{O}_1}{2} \\ &= -\epsilon_e \frac{|\tilde{L}_{1\alpha}|}{|L_{\alpha}|}. \end{aligned} \quad (34)$$

In assembling all elements together, the resulting element coefficients for the two adjacent triangles, 1 and 2, sharing the line L_{α} are added together such that

$$C_{FEM}(i, j) = -\left(\epsilon_1 \frac{|\tilde{L}_{1\alpha}|}{|L_{\alpha}|} + \epsilon_2 \frac{|\tilde{L}_{2\alpha}|}{|L_{\alpha}|} \right). \quad (35)$$

Equation (35) is equivalent to (20) with the average permittivity defined as in (21). We can conclude:

The coefficient matrix resulting from a finite formulation with a Voronoi dual mesh is equal to the coefficient matrix resulting from a FEM formulation with linear shape functions for the same triangular mesh.

4.4.2 Charge vectors

With the choice of a uniform charge density in each primal element, it was shown that the charge vector for the FEM approach (30) is equal to the charge vector for a barycentric dual mesh as was shown in Fig. 14. The charge vector for Finite Formulation (19) is equal to the charge vector for a Voronoi dual mesh as was shown in Fig. 11. Coefficient matrices for both methods (20, 35) can be derived from a Voronoi dual mesh and, as shown previously, are the same. If the charge density is zero (Laplace's equation), the two methods are exactly equivalent. However, for a non-zero charge density Cell Method produces locally more accurate results, especially for coarse meshes. The difference between the charge matrices in the two methods is indicated in Fig. 16 and vanishes for finer meshes. For a coarse mesh and for abrupt changes in charge density, The Cell Method solution should be more accurate.

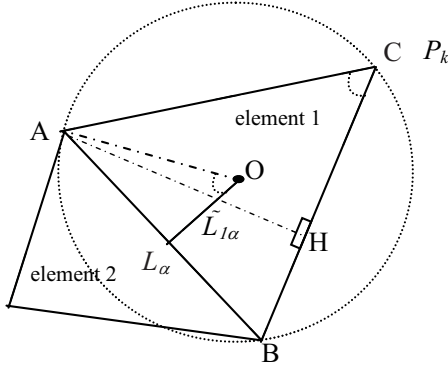


Figure 15: Circumcircle of element 1. O is the circumcenter of triangle ABC and AH is the altitude from vertex A .

In the case of a continuous charge density function, Cell Method can easily use the charge density at each primal point for the dual area surrounding that point. In the FEM we still need to assume a constant charge density or employ interpolation (linear or higher order) to approximate the charge density inside primal elements.

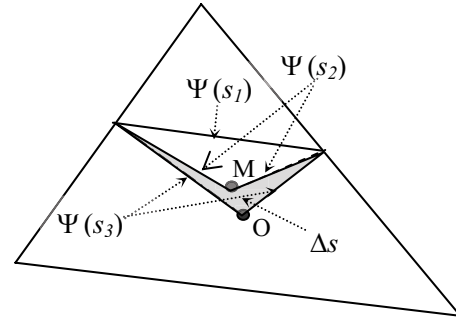


Figure 16: The difference between the charge vectors in the FEM and Finite Formulation. M is the barycenter (FEM) and O is the circumcenter (FF) of the triangle. The electric flux entering the (extruded) surface, $\Psi(s_1)$, will be equal to the fluxes leaving, $\Psi(s_2)$ and $\Psi(s_3)$, if there is no charge in the enclosed surface. In general $\Psi(s_3) - \Psi(s_2) = Q(\Delta_s)$.

5 Example

A GaAs Schottky Barrier Diode with a non-uniform doping profile has been chosen as an example for comparing Cell Method and Finite Element Method. The simplified geometry is shown in Fig. 17. The computational mesh consists of 10 by 5 (or 6 by 3) squares in x and y directions, respectively. Each of the squares is diagonally divided into two triangles over the half geometry in order to make use of symmetry. The continuous and discretized charge density profiles are shown in Fig. 18 for the mesh with five elements in the y direction. The resulting potential on the middle cross-section shown in Fig. 17 is given in Fig. 19. Figure 19 indicates a small difference between the solution resulting from FF and FEM in the case of the coarse mesh. For the finer mesh the difference almost vanishes. FEMLAB 3.1, COMSOLAB www.comsol.com, uses a fine mesh and higher order elements and the difference between two FEMLAB solutions is a result of discretizing the charge density profile.

6 Conclusion

The Cell Method, a finite formulation technique was compared in detail with the Finite Element Method. Starting from a topological background,

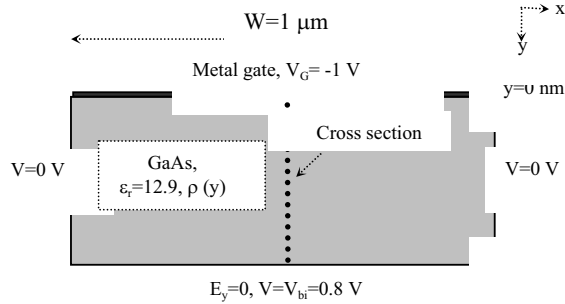


Figure 17: Simplified geometry of a Schottky diode on a doped GaAs substrate.

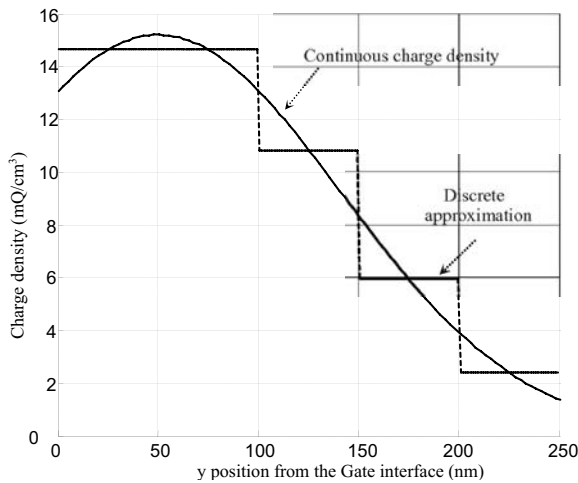


Figure 18: Non-uniform doping profile and the discretized charge density function for five elements in y direction.

electrostatic laws were formulated in both differential and finite frameworks. A geometrical proof showing the equivalence of the coefficient matrices in the two methods was given.

It was shown that, even though the finite element technique does not explicitly use a dual mesh, assuming linear shape functions and uniform charge density in each element, is equivalent to the use of a barycentric dual mesh for the charge vector and Voronoi dual mesh for the coefficient matrix. Cell Method on the other hand, produces a coefficient matrix and a charge vector that are both based on the Voronoi dual mesh. As a conclusion, different shape functions produce different weighted averages for permittivity and charge density functions over each element, which is equivalent to the con-

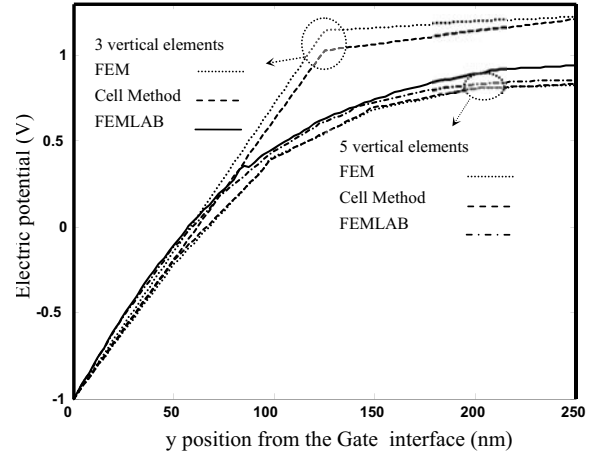


Figure 19: Electric potential on the cross section shown in Fig. 17, for using two different mesh sizes are compared with the solution using FEM-LAB.

struction of different dual meshes in finite formulation. It should be noted that dividing square elements diagonally into two triangles is not a proper way for mesh refinement as the coefficient relating two nodes on a diagonal line is zero.

The emphasis in this work was to show that a direct finite formulation technique, which starts from physical laws as topological relations, results in the same set of linear algebraic equations as a variational technique .

Acknowledgement: This work was supported by the Natural Sciences and Engineering Research Council of Canada (NSERC) and a Manitoba Hydro research grant.

References

Araneo, R. (2002): Numerical Solution of Transient Electromagnetic Scattering Problems Using the Novel Time-Domain Cell Method. *IEEE International Symposium on Electromagnetic Compatibility*.vol.1, pp.291-29.

Bettini, P.; Trevisan, F. (2003): Electrostatic Analysis for Plane Problems with Finite Formulation. *IEEE Trans. on Magnetics*, vol. 39, no.3.

Bellina, F.; Bettini, P.; Tonti, E. and Trevisan, F. (2002): Finite Formulation for the Solution of

a 2-D Eddy-Current Problem. *IEEE Trans. on Magnetics*, vol.38, no.2.

Bossavit, A. (1998): How weak is the weak solution in finite element method? *IEEE Trans. on Magnetics*, vol. 34, no. 5.

Bossavit, A.; Kettunen, L. (2000): Yee-Like Schemes on Staggered Cellular Grids: A Synthesis between FIT and FEM approaches. *IEEE Trans. On Magnetics.*, vol. 36, no.45.

Christopoulos, C. (1995): *The Transmission Line Modeling Method, TLM*. IEEE Press.

Clemens, M.; Weiland, T. (2001): Discrete electromagnetism with the finite integration technique. *PIER32*, pp. 65-87.

COMSOLAB, www.comsol.com.

Cosmi, F. (2005): Elastodynamics with the Cell Method, *CMES: Computer Modeling in Engineering and Sciences*, vol. 8, no. 3, pp. 191-200.

Harrington, R. F. (1961): *Time-Harmonic Electromagnetic Fields*, McGraw-Hill.

Marrone, M.; Mitra, R. (2004): A Theoretical Study of the Stability Criteria for Generalized FDTD Algorithms for Multiscale Analysis. *IEEE Trans. on Antennas and propagation*. vol. 52, no. 8.

Marrone, M. (2002): Novel Numerical method for the analysis of 2D photonic crystals: the cell method. *Optics Express*, vol. 10, no. 22.

Marrone, M.; Frasson, A. M. F. and Figueroa, H.E.H. (2002): A Novel Numerical approach for electromagnetic Scattering: The Cell Method. *Proceedings, IEEE AP-URSI*.

Marrone, M; Grassi, P. and Mitra, R. (2004): A new technique based on the Cell Method for calculation the propagation constant of inhomogeneous filled waveguide. *International Symposium on Antenna and propagation, IEEE*.

Mattiussi, C. (2000): An analysis of finite volume, finite element and finite difference methods using some concepts from algebraic topology. *Advances in Imaging and Electron Physics*, vol. 113, pp.1-146.

Miller, E.K. (1998): A Selective Survey of Computational Electromagnetics. *IEEE Trans. on Antenna and Propagation*, vol. 36, no. 9. pp.1281-

1305

Marrone, M. (2001): Computational Aspects of the Cell method in Electrodynamics. *PIER 32*, pp. 317-356.

Repetto, M.; Trevisan, F. (2003): 3-D Magneto-statics with Finite Formulation. For the Solution of 3D nonlinear Magnetostatic. *IEEE Trans. on Magnetics*. vol. 39, no.3.

Sadiku, M. N. O.; Makki, A. Z. and Agba, L. C. (1991): A further introduction to finite element analysis of electromagnetic problems. *IEEE Transion Education*, vol. 34, no. 4.

Silvester, P. P.; Ferrari, R. L. (1990): *Finite Element for Electrical Engineers*. Cambridge University Press.

Specogna, R.; Trevisan, F. (2005): Discrete Constitutive Equations in A- χ Geometric Eddy-Current Formulation. *IEEE Trans. on Magnetics*. vol. 41, no.4.

Straface, S.; Troisi, S. and Gagliardi, V. (2006): Application of the Cell Method to the Simulation of Unsaturated Flow, *CMC: Computers, Materials and Continua*, vol. 3, no. 3, pp. 155-166.

Taflove, A. (1995): *Computational Electrodynamics*. Artech House.

Tonti, E. (2001): A direct discrete formulation of field laws: the Cell Method. *CMES: Computer Modeling in Engineering and Sciences*, vol.2, no.2, pp. 237-258.

Trevisan, F.; Kettunen, L. (2004): Geometric Interpretation of Discrete Approaches to Solving Magnetostatics. *IEEE Trans. on Magnetics*. vol. 40, no.2.